Scalable Synthesis of an Architectural Library of Well-Defined Poly(Acrylic Acid) Derivatives: Role of Structure on Dispersant Performance

David J. Lunn,[1,2] Sungbaek Seo,[1,3] Sang-Ho Lee,[1] Raghida Bou Zerdan,[1] Kaila M. Mattson,[1,4,6] Nicolas J. Treat,[1,4] Alaina J. McGrath,[1] Will R. Gutekunst,[1] Jimmy Lawrence,[1] Allison Abdilla,[1] Athina Anastasaki,[1] Abigail S. Knight,[1] Bernhard V. K. J. Schmidt,[1,4] Morgan W. Bates,[1] Paul G. Clark,[6] Jonathan P. DeRocher,[7] Antony K. Van Dyk,[7] Craig J. Hawker [1,4,5]

[1]Materials Research Laboratory, University of California Santa Barbara, Santa Barbara, California 93106
[2]Department of Chemistry, University of Oxford, Oxford OX1 3TA, United Kingdom
[3]Department of Biomaterials Science, Pusan National University, Miryang 50463, Republic of Korea
[4]Department of Chemistry and Biochemistry, University of California Santa Barbara, Santa Barbara, California 93106
[5]Materials Department, University of California Santa Barbara, Santa Barbara, California 93106
[6]The Dow Chemical Company, Midland, Michigan 48674
[7]Dow Coating Materials, The Dow Chemical Company, Collegeville, Pennsylvania 19426
Correspondence to: A. K. Van Dyk (E-mail: avandyk@dow.com) and C. J. Hawker (E-mail: hawker@mrl.ucsb.edu)

Received 1 November 2018; accepted 11 December 2018; published online 10 January 2019
DOI: 10.1002/pola.29316

ABSTRACT: The synthesis and systematic comparison of a comprehensive library of well-defined polymer architectures based on poly(acrylic acid) is reported. Through the development of new synthetic methodologies, linear, single branched, precision-branched comb, and star polymers were prepared and their performance as dispersants was evaluated. The ability to accurately control chain lengths and branch points allows the subtle interplay between structure and dispersant performance to be defined and affords critical insights into the design of improved polymeric additives for coating formulations. The general industrial relevance of ionic polymers and branched macromolecular architectures supports these design rules for a wide range of other applications and materials, including as additives for personal care products and in water treatment. © 2019 Wiley Periodicals, Inc. J. Polym. Sci., Part A: Polym. Chem. **2019**, *57*, 716–725

KEYWORDS: controlled branching; dispersants; poly(acrylic acid); polymer architectures; polymeric additives; scalable synthesis

INTRODUCTION Architecture and branching are key design features of polymeric materials that significantly influence material properties and play a major role in facilitating important industrial processes.[1–3] As an illustrative example, polyethylene, one of the simplest and most widely used commodity polymers, can be either a high strength or ductile material, depending on the degree of backbone branching.[4] Significantly, solubility, crystallinity, and morphology are also dictated by polymer architecture.[5–12] While a systematic understanding of the influence of these structural features on polymer properties would be highly beneficial, studies that tune and compare architectural isomers are synthetically challenging.

The development of controlled polymerization techniques has facilitated the synthesis of complex polymer architectures.[13,14] Synthetic strategies have been developed for the preparation of architectures ranging from linear polymers to high-molecular-weight dendritic structures.[3] Recent studies illustrate the promise of discrete macromolecules in a range of applications ($Đ$ = 1).[15,16] For example, discrete macromolecules are desirable for fundamental understanding of dispersant performance since minor deviations from the targeted molecular weight and chain-end nature can significantly influence material properties/performance.

Herein, we report the efficient and scalable synthesis of a comprehensive library of poly(acrylic acid) (PAA) architectures for use as polymeric dispersants. While industrially important, structure–property relationships for dispersants are not well developed due to the complex nature of the overall system. For example, in paint and coating formulations, water soluble polymer additives are used to modify the properties of both inorganic pigments (e.g., titanium dioxide, TiO_2)

Additional supporting information may be found in the online version of this article.

†David J. Lunn and Sungbaek Seo contributed equally to this work.

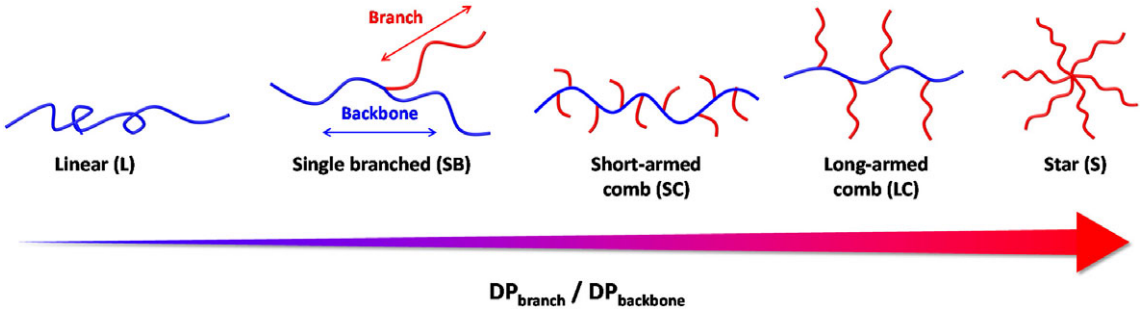

FIGURE 1 Overview of the five target PAA architecture types identified by the DoE model. Blue colored segments represent the polymer backbone and red colored segments denote polymer branches. See Table 1 for structural characterization and Supporting Information Figure S1 for a representation of all 16 PAA architectures. [Color figure can be viewed at wileyonlinelibrary.com]

and filler particles (e.g., calcium carbonate, $CaCO_3$), with the specific aim of achieving uniform dispersions, improving particle stability, and increasing the dispersant efficiency. A fundamental understanding of the structural parameters that influence the adsorption of macromolecules onto the surface of TiO_2 is also of particular interest,[17–25] given the favorable optical properties and high cost of the TiO_2 pigment particles. A systematic study examining the influence of branching and molecular weight on the dispersion of TiO_2 would therefore offer new design rules for the preparation of high-performance dispersants. In this study, the selection of macromolecular targets was driven by a statistical design of experiment (DoE) model, which allows for the maximization of structural variety and the elucidation of structure–property trends (Fig. 1). The knowledge gained from this study will permit the development of design rules for next generation polymer additives for paint formulations, personal care products, and water treatment.

EXPERIMENTAL

See Supporting Information for all experimental procedures and polymer characterization data.

RESULTS AND DISCUSSION

Synthesis of PAA Architectures

In total, five distinct PAA architectures (16 samples in total) were targeted based on a statistical DoE model—three linear (L), four single branched (SB), four short-armed comb (SC), four long-armed comb (LC), and a six-arm star (S), with total degrees of polymerization (DP_n) of 30, 60, or 120 repeat units. In addition, the architectural diversity in these materials maximizes the design space that can be investigated, offering significant insight into structural features that influence the performance of polymers as pigment dispersants. In addition, a major advantage of this statistical approach lies in the elucidation of a systematic correlation between polymer structure and function, enabling predictions to be made about the properties of new dispersant architectures. The target architectures can be categorized by either structural features (linear, branched, etc.) or total DP_n (30, 60, or 120 repeat units), with the degree of branching, defined as the ratio of the total DP_n of branches to the DP_n of the main polymer backbone ($DP_{branch}/DP_{backbone}$), being of particular interest (Fig. 1).

A major goal of this study was the development of scalable synthetic approaches to tunable PAA architectures with accurate control over branching, chain-ends, dispersity, and total DP_n. To facilitate the purification and characterization of these PAA materials, all architectures were first prepared as *tert*-butyl esters and subsequently deprotected to afford the desired PAA analogues (Schemes 1–5). Initially, anionic[26] and nitroxide-mediated[27] polymerizations were examined; however, the need for stringent reaction conditions or challenges associated with acrylate-based monomers precluded their successful use. While reversible addition-fragmentation chain

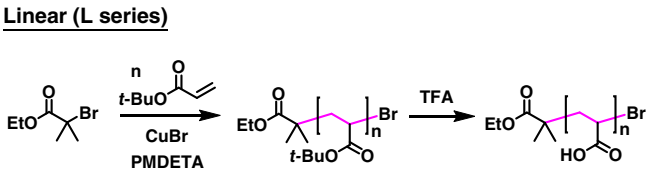

SCHEME 1 General synthetic route to linear PAA architectures (L series). [Color figure can be viewed at wileyonlinelibrary.com]

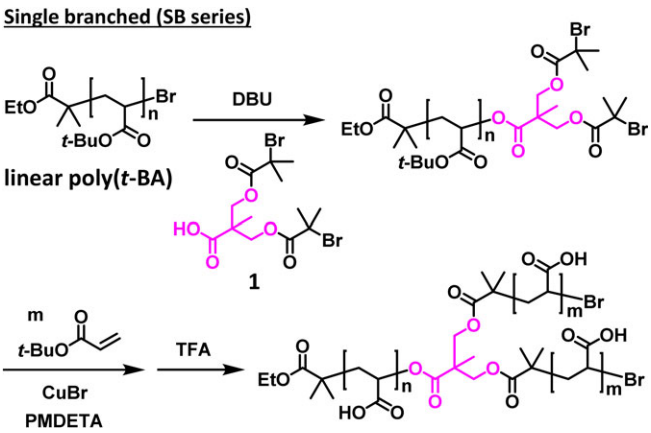

SCHEME 2 General synthetic route to single branched PAA architectures (SB series). [Color figure can be viewed at wileyonlinelibrary.com]

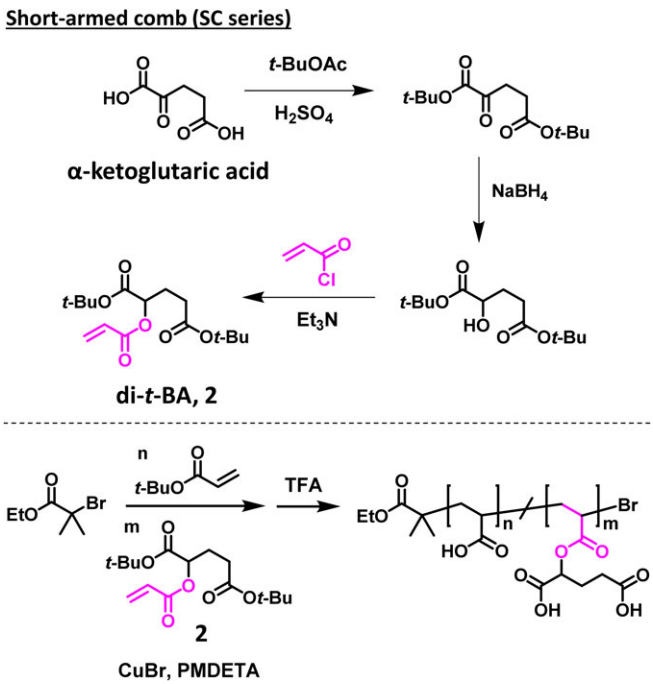

SCHEME 3 General synthetic route to short-armed comb PAA architectures (SC series). Synthesis of di-*t*-BA from α-ketoglutaric acid (top) and copolymerization of *t*-BA and di-*t*-BA (bottom). [Color figure can be viewed at wileyonlinelibrary.com]

transfer (RAFT)[28] polymerization techniques were shown to be more user-friendly approach for the controlled polymerization of acrylates, the presence of linear polymer impurities in RAFT systems decreases the architectural integrity for the branched derivatives. As a result, atom transfer radical polymerization (ATRP)[29,30] was chosen as the primary polymerization strategy for the synthesis of linear polymers as well as complex architectures such as star[31] and comb[32] structures.

Linear poly(*t*-butyl acrylate) polymers with different degrees of polymerization, DP_{30} (L1), DP_{60} (L2), and DP_{120} (L3), were therefore prepared using well-established copper-catalyzed ATRP conditions to give linear poly(*t*-BA) with low-molecular-weight distributions ($Đ < 1.2$) (Scheme 1). Importantly, nuclear magnetic resonance (NMR) spectroscopy and gel permeation chromatography (GPC) showed excellent agreement between theoretical and experimental values, confirming the high degree of structural control over these materials (Table 1, entries L1, L2, and L3, Supporting Information Figs. S2–S10).

For the single branched AB_2 stars (SB series), where A and B represent PAA segments of different DP_n, our initial strategy focused on a modular, convergent approach. In this strategy, the polymer backbone (i.e., B_2 segment) was prepared from a dual ATRP initiator bearing two bromides and one terminal alkyne unit. Copper-catalyzed azide-alkyne cycloaddition was then employed to attach an azide terminated poly(*t*-BA) branch (A) to the middle of the B_2 chain via conjugation with the specifically placed alkyne side chain. However, all attempts at coupling resulted in generation of a high molecular weight shoulder in the GPC traces, which was attributed to side reactions involving Glaser coupling.[33,34] As an alternative, we employed a divergent approach where a linear *t*-BA chain (A) was initially grown from a monofunctional initiator and the terminal bromide displaced with the carboxylic acid **1** containing two bromide initiator moieties already installed (Scheme 2).

The highly efficient nature of the DBU chemistry coupled with orthogonal displacement of the secondary bromide over the two tertiary bromides allows for the direct formation of a difunctional macroinitiator. Symmetrical chain extension from a single branch point afforded the desired AB_2 based on initial linear chains (A) of DP_n = 2, 10, 22, and 74 and B_2 chain of DP_n = 26, 50, 8, and 42 (overall DP_n of 30, 60, 30, and 120 acrylic acid units, respectively). All macromolecules were fully characterized using a combination of spectroscopic and chromatographic techniques with excellent agreement between theoretical/experimental DP_n and low dispersities being observed in all cases (Table 1, entries SB1, SB2, SB3, and SB4, Supporting Information Figs. S11–S24).

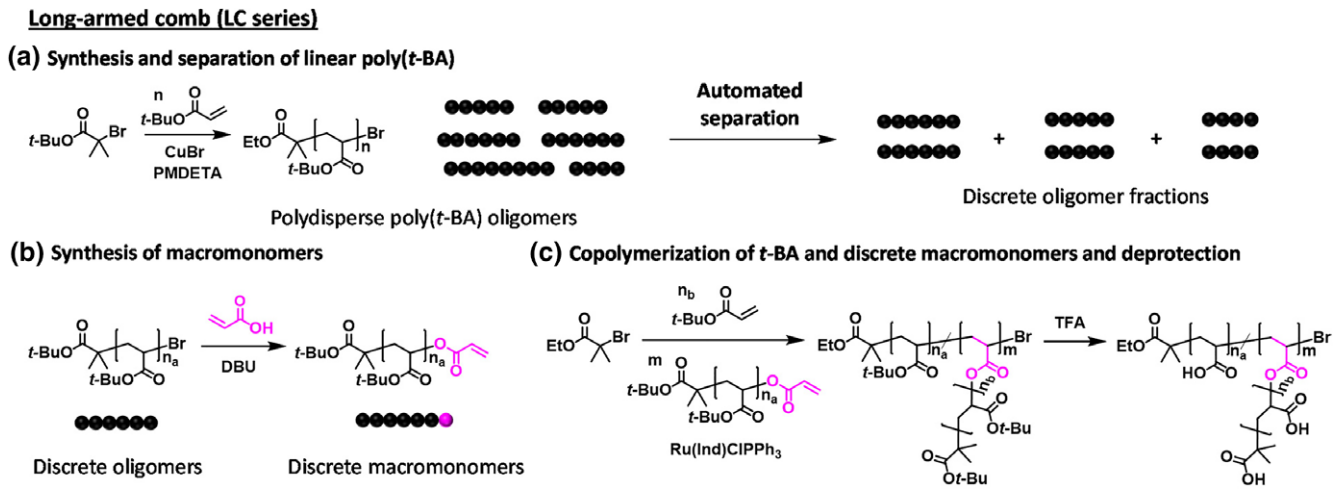

SCHEME 4 General synthetic route to long-armed comb PAA architectures (LC series) [Color figure can be viewed at wileyonlinelibrary.com]

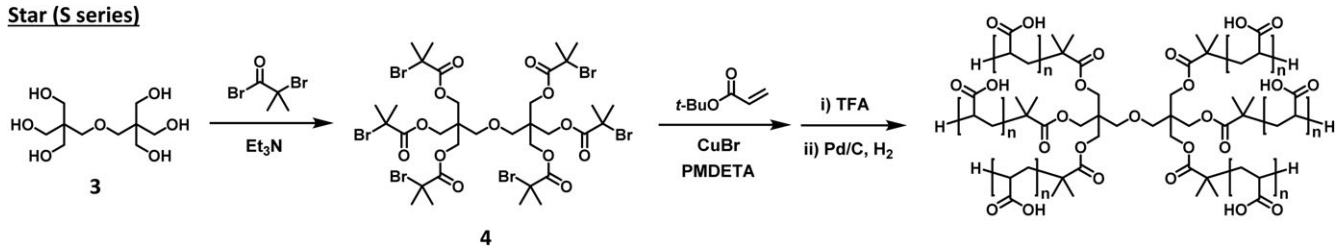

SCHEME 5 General synthetic route to six-arm star PAA architectures (S series).

The short-armed comb architectures (SC series) identified by the DoE model contain branches of DP_n = 2 with varying backbone lengths. These short chain lengths necessitated the development of a novel di-*tert*-butyl acrylate monomer **2** (di-*t*-BA, Scheme 3), which was prepared from inexpensive, commercially available ketoglutaric acid.[35] Comparable reactivity ratios with *t*-BA and negligible differences between the observed incorporation and initial feed ratio of the two monomers allows well-defined copolymers to be prepared by ATRP.[35] When deprotected, the incorporated di-*t*-BA monomer resembles a precise DP_2 branch of PAA, resulting in a series of short-chain copolymers with varying di-*t*-BA incorporation and accurate control of the overall DP_n (polymers with backbone DP_n of 15, 39, 61, and 100, containing 6, 10, 13, and 31 branches, respectively) (Table 1, entries SC1, SC2, SC3, SC4, Supporting Information Figs. S25–S36).

For the synthesis of the long-chain PAA comb materials (LC series), a similar level of control over branch length was desired. Unfortunately, conventional living polymerization techniques (e.g., anionic, ATRP, RAFT, etc.) give rise to statistical distributions and due to the low degrees of polymerization targeted for these branches (DP_n = 4, 6, 8, and 15), minor disparities in branch lengths significantly influence the final properties, obscuring any structural trends.[36–38] For these reasons, preparing oligomonomers of precise DP_n ($Đ$ = 1) was of utmost importance and our recent development of a scalable separation strategy for the isolation of discrete oligomers

TABLE 1 Structural Characterization of Dispersant Architectures

	Backbone	Branches		Total		
Structure	DP_n[a]	#Branches	DP_n[a]	DP_n[a]	M_n (g/mol)[b]	$Đ$[c]
Linear (L)						
L1	32 (30)	–	–	32 (30)	4000	1.13
L2	57 (60)	–	–	57 (60)	5900	1.13
L3	120 (120)	–	–	120 (120)	9700	1.13
Single branched (SB)						
SB1	22 (20)	2	4 (5)	36 (30)	3800	1.15
SB2	2 (2)	2	13 (14)	27 (30)	4400	1.17
SB3	74 (80)	2	21 (20)	117 (120)	9500	1.21
SB4	10 (8)	2	25 (26)	60 (60)	6900	1.19
Short comb (SC)						
SC1	15 (12)	10 (9)	2	35 (30)	3700	1.18
SC2	39 (36)	13 (12)	2	65 (60)	9200	1.13
SC3	61 (60)	31 (30)	2	123 (120)	12,100	1.12
SC4	100 (108)	6 (6)	2	112 (120)	12,200	1.21
Long comb (LC)						
LC1	9 (6)	4 (4)	6	34 (30)	4400	1.28
LC2	20 (15)	3 (3)	15	72 (60)	5900	1.25
LC3	21 (18)	3 (3)	4	32 (30)	4700	1.37
LC4	27 (24)	12 (12)	8	125 (120)	4800	1.39
Star (S)						
S1	-	6	5 (5)	30 (30)	3600	1.16

Structural analysis of intermediate *t*-BA polymers by ^{1}H NMR[a] and GPC[c]. [b]PAA molecular weights were calculated from the obtained DP_n of P(*t*-BA). Brackets denote the target DP_n identified by the DoE model. See Supporting Information for experimental procedures and full polymer characterization.

utilizing automated silica gel chromatography proved to be key.[15] Initially, oligomerization of *t*-BA by ATRP was carried out from an initiator bearing an alcohol unit which would allow subsequent esterification with acryloyl chloride to afford the desired α-vinyl oligomonomer. However, due to the polarity of the alcohol chain end, oligomer separation proved challenging. To circumvent this, *tert*-butyl 2-bromoisobutyrate was selected as a non-polar protected initiator to aid oligomer separation. This initiator has an additional advantage in that it resembles a terminal acrylic acid repeat unit after final deprotection, but necessitates that the acryloyl group be introduced at the ω-chain end. To this end, polymerization from *tert*-butyl 2-bromoisobutyrate afforded multigram quantities of crude oligomeric *t*-BA which could be separated into fractions of discrete lengths ($Đ$ = 1) (Supporting Information Figs. S37 and 38). The bromide chain-ends were then substituted with acrylic acid in the presence of 1,8-Diazabicyclo[5.4.0]undec-7-ene, allowing quantitative introduction of a terminal acrylate unit and giving scalable quantities of the desired discrete oligomonomers with DP_n of 4, 6, 8, and 15 (Supporting Information Figs. S39–S42).

While copper-catalyzed copolymerization of the oligomonomers proved to be efficient for the synthesis of comb copolymers with short branches (DP_4 and DP_6), inefficient conversion of the oligomonomers was observed for those with higher molecular weight chains (DP_8 and DP_{15}), resulting in broad molecular weight distributions. In contrast, copolymerizations catalyzed by Ru(Ind)ClPPh$_3$ (Ind = indole), in the presence of tributylamine yielded high conversions of even the longest oligomonomers (DP_{15}) (Scheme 4, Supporting Information Figs. S43–S50). In all cases, copolymerizations were monitored by NMR and GPC, which showed near-ideal random copolymerization of both *t*-BA and the oligomonomers, affording a library of long-chain combs with the number and length of the grafted arms being accurately controlled by tuning the monomer feed ratio and the initial DP_n of the discrete oligomonomers. Comb architectures with backbone DP_n of 9, 20, 21, and 27, with 4, 3, 3, and 12 branches (DP_n = 6, 15, 4, and 8, respectively) were prepared on multigram scale for dispersant performance testing, in excellent agreement with the DoE targets (Table 1, entries LC1, LC2, LC3, and LC4).

The final architecture identified by the DoE model was a six-arm star polymer,[39] which was prepared from a hexafunctional initiator using a traditional "grafting-from" approach (Scheme 5). Short ATRP reaction times and low conversions were targeted to minimize chain–chain coupling leading to a star polymer with arms of average DP_5 (target DP_n of 5) and overall low dispersity ($Đ$ < 1.2) (Table 1, entry S1, Supporting Information Figs. S56 and S57). To negate any influence of chain-ends, the bromide end-groups were removed through a simple and quantitative hydrogenation protocol recently developed in our group.[40] As detailed in the Supporting Information, full structural analysis of intermediate *t*-BA polymers was accomplished by ^{1}H NMR and GPC with PAA molecular weights calculated from the obtained DP_n of the corresponding P(*t*-BA) derivatives (Table 1).

PAA Architectures as TiO_2 Pigment Dispersants

The availability of a library of macromolecular architectures with controlled DP_n and well-defined branching enables structure–property relationships to be developed for dispersion performance. As an industrially important benchmark, the performance of these PAA derivatives as polymeric dispersants for TiO_2 pigment in paint and coating applications was studied. In all cases, the branched PAA derivatives were compared to linear controls while the reduction in flocculation and overall viscosity (η) of the system were examined (Fig. 2).[17] The TiO_2 selected for this study is widely utilized in paint and coating formulations (marketed by DuPont under the trade name Ti-Pure® R-706), with a median size of 360 μm and surface layers of silica and alumina that facilitate both durability and dispersion. To allow for comparison with commercial PAA-based dispersants that operate at slightly basic pH, all 16 PAA architectures were dissolved in water, adjusted to pH 10 using sodium carbonate, purified by dialysis, and isolated as white powders after freeze-drying. In all cases, aqueous solutions of the purified and redissolved NaPA architectures were found to have a pH of ~9.

Dispersant demand plots were obtained for each polymer architecture by measuring the viscosity of aqueous TiO_2 slurries with different dispersant amounts. The viscosity of aqueous dispersions of 70 wt % TiO_2 containing between 0 and 1.5 wt % linear PAA dispersants (L1, L2, and L3) was measured using a parallel plate rheometer at a constant shear rate of 100 s^{-1} and compared with commercially available linear PAA (M_w ~ 15,000 g mol^{-1}) (Supporting Information Fig. S59). The viscosity of the particle slurry was observed to be highly dependent on the molecular weight as well as the added weight percentage of dispersant. To compare the dispersant performance of our linear architectures, we chose to focus on lower dispersant amounts (0.0–0.1 wt %), where a molecular weight influence on the viscosity of TiO_2 slurries is more clearly observed.[41–44] For the linear dispersants (L series), as the molecular weight of the PAA polymer increases, an increasing amount is required to reach a minimum plateau viscosity [Fig. 3(a)]. This change in dispersion performance with degree of polymerization could also be clearly illustrated by examining the viscosity at a specific dispersant amount. For example, addition of 0.05 wt % of L1 (DP_{30}) results in a

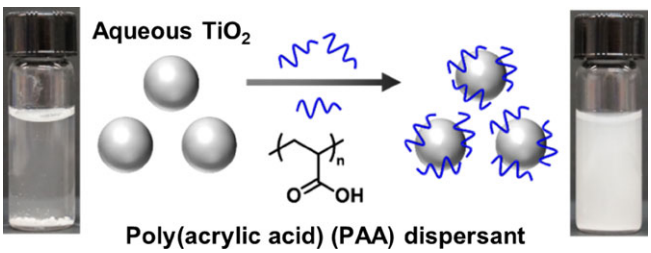

FIGURE 2 Schematic representation of the dispersion of TiO_2 pigment particles by PAA dispersants. TiO_2 powder (left image) is stabilized in water via adsorption of PAA onto the particle surfaces, affording a stable suspension (right image). [Color figure can be viewed at wileyonlinelibrary.com]

fluid TiO_2 dispersion (η = 0.4 ± 0.1 Pa s), while 0.05 wt % of L2 (DP_{60}) or L3 (DP_{120}) results in pastes (η = 1.3 ± 0.1 Pa s and η = 1.9 ± 0.3 Pa s, respectively). Importantly, significant reductions in viscosity were observed for all controlled molecular weight linear systems in comparison with the commercial derivative (DP_{200}, 15,000 g mol^{-1}), which afforded a powder (η ~ 3.1 Pa s) (Fig. 3).

The influence of dispersity on the performance of PAA-based dispersants was then investigated with samples of similar DP_n by comparing L1 ($Đ$ 1.1; DP_n = 30) to a commercial sample of polydisperse PAA ($Đ$ 2.4; DP_n = 30). Significantly, addition of L1 to a TiO_2 particle slurry results in a reduced viscosity when compared to the polydisperse PAA sample [Fig. 3(b)]. For control experiments, a comparable dispersant demand plot was elucidated for both a PAA-based commercial paint additive (TAMOL 945®) and sodium acetate [Fig. 3(b)]. The polymeric dispersants had enhanced performance relative to the small molecule analogue with a trend of decreasing $Đ$ leading to improved performance, consistent with previous reports.[42] A rationale for this behavior is that the adsorption of linear PAA onto a variety of substrates and surfaces[41–52] occurs through a combination of both electrostatic and steric forces,[53–58] where the effective dispersion of particles is driven by the ability of a polymer to adopt loop conformations on a particle surface [Fig. 4(a)].[54] However, PAA chains with increased DP_n are more likely to bridge particles than adopt a loop conformation [Fig. 4(b)], causing pigment flocculation and increasing the overall viscosity of the system. As a result, dispersants with increased $Đ$ contain fractions of both lower and higher molar mass PAA, providing inadequate surface adsorption or bridging between particles, respectively. Both factors contribute to colloidal instability.[41]

Having demonstrated the importance of molecular weight (DP_n) and $Đ$ for tuning the dispersion performance of linear PAA, we next sought to identify architectural features that would further increase dispersing ability. As before, a focus

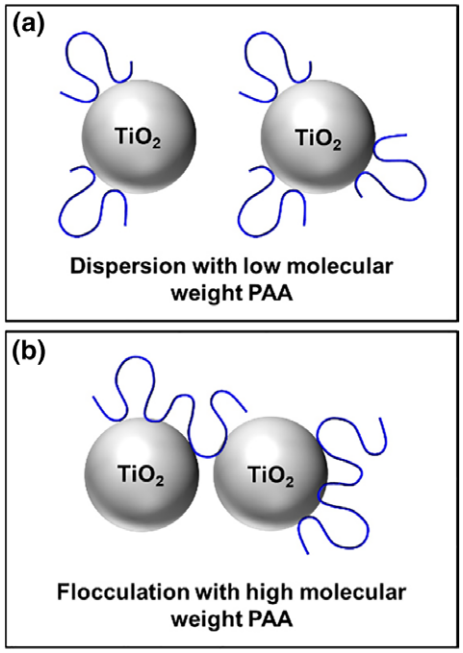

FIGURE 4 Cartoon representation of dispersion (a) and flocculation (b) of TiO_2 particles with low and higher molecular weight linear PAA, respectively. [Color figure can be viewed at wileyonlinelibrary.com]

on low dispersant loadings (0.0–0.1 wt %) enables the differences due to architecture to be more clearly distinguished.

Dispersant demand plots for the lowest DP_n series of PAA architectures (DP_{30}) were obtained between 0.0 and 0.1 wt % PAA (Fig. 5). Structurally, SB2 was designed to have a single short branch from the mid-point of the polymer backbone, making it an almost identical material to L1. Accordingly, the rheological properties of L1 and SB2 showed negligible differences and indicated that a short central branch does not significantly influence dispersant performance. However, the

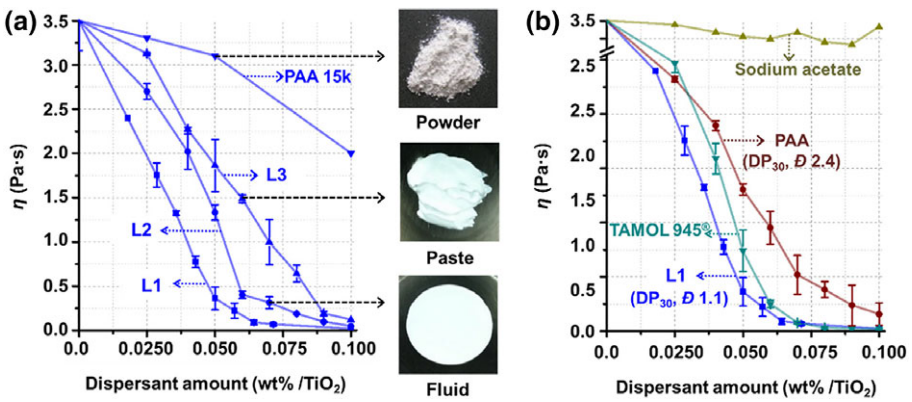

FIGURE 3 Dispersant demand plots of aqueous TiO_2 dispersions versus PAA dispersant amount (0–0.1 wt %/TiO_2): (a) influence of molecular weight and (b) influence of dispersity on viscosity. Viscosities were measured at a shear rate of 100 s^{-1}. Lower constant shear rates (<100 s^{-1}) lead to large differences in viscosity due to the shear-thinning behavior of aqueous TiO_2 dispersions. The two commercially available PAA materials used were DP_{200} ($Đ$ > 2, Sigma Aldrich) and DP_{30} ($Đ$ = 2.4, Polyscience). [Color figure can be viewed at wileyonlinelibrary.com]

introduction of additional short branches of DP_n 2 (SC1), 4 (LC3), and 5 (S1) into the PAA architectures, while maintaining the total DP_{30}, was observed to increase dispersion viscosity. This is most likely due to the steric hindrance from the branch points that impede the main polymer backbone from adopting a loop confirmation on the surface, while the DP_n of the attached branches themselves are too low to bind independently. In support of this hypothesis, the viscosities of dispersions prepared from DP_{30} architectures with fewer and slightly longer branches (SB1 and LC1) were found to be intermediate between that of the linear and highly branched materials.[42,59]

In order to correlate the performance of these dispersants, isothermal titration calorimetry (ITC) was used to calculate the binding constant (K_a), enthalpy changes (ΔH), and thermodynamic parameters for the interaction between different PAA architectures and the surface of TiO_2 particles.[60,61] Importantly, comparing different polymer architectures with the same DP_n eliminates molecular weight effects and allows the influence of structure on dispersant performance to be probed. Titration of sub-stoichiometric amounts of each PAA derivative into an aqueous suspension of TiO_2, allowed endotherms ($\Delta H > 0$), attributed to the direct binding interactions (adsorption) to the particle surfaces, to be observed for all polymeric architectures (Supporting Information Fig. S61). From the resulting heat flow data, an adsorption model was used to calculate the thermodynamic parameters for the interaction between the different PAA architectures and TiO_2 (Supporting Information Table S7). Significantly, a linear trend was observed between binding affinity and dispersant performance (TiO_2 slurry viscosity at 0.05 wt % PAA) with the

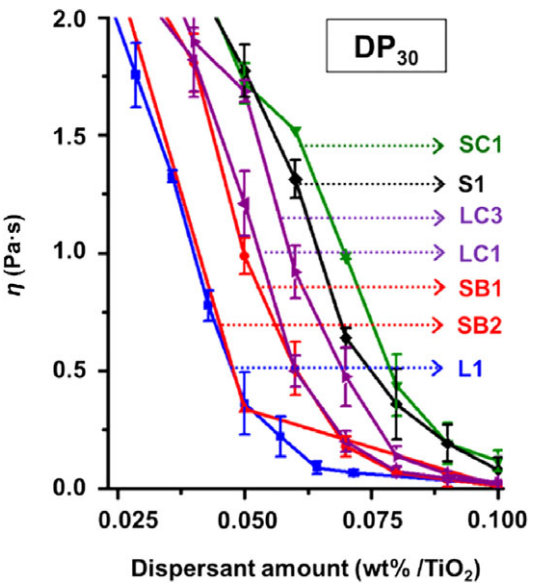

FIGURE 5 Dispersant demand plots of aqueous TiO_2 dispersions versus PAA dispersant amount. Effect of architecture within the same DP_{30} series. Viscosities were measured at a constant shear rate of 100 s^{-1}. [Color figure can be viewed at wileyonlinelibrary.com]

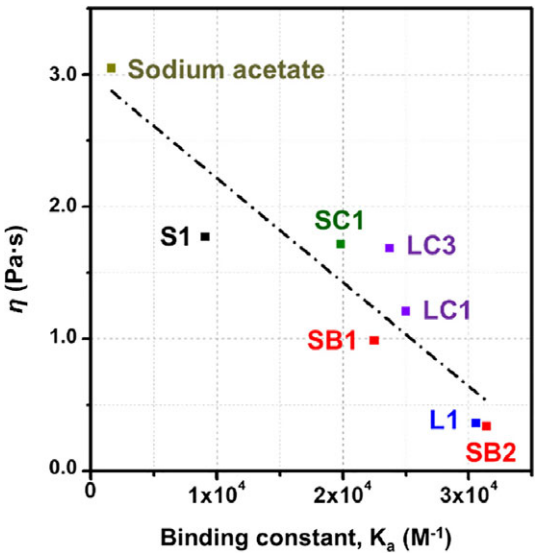

FIGURE 6 Viscosity of TiO_2 particle dispersions versus binding constant of PAA-TiO_2 particle adsorption for DP_{30} series. [Color figure can be viewed at wileyonlinelibrary.com]

higher binding constants correlating with increased dispersing capability (Fig. 6). As demonstrated above for the dispersant demand plots, the binding constant for the linear polymer (L1) and the corresponding derivative with a single short branch (SB2) were essentially identical. Architectures with intermediate branching (SB1, SC1, LC1, and LC3) were observed to have lower binding constants with the lowest binding constant being observed for the star architecture (S1). The binding constant for all of the polymeric dispersants was significantly greater than for the small molecule control, NaOAc ($K_a = 1.6 \times 10^3$ M^{-1}), confirming the importance of multiple binding groups in these systems.[62]

The power of using a range of macromolecular isomers with similar degrees of polymerization and different architectures is that by comparing the ITC data, we can propose that the binding constant is influenced by a polymer's ability to rearrange to maximize the number of favorable interactions with the particle surface, reducing displacement, and enhancing steric stabilization. Through evaluation of the DP_{30} architectures, the trend observed for both binding constant and dispersion viscosity is related to the structural features of the polymers. For example, linear PAA (L1) is only restricted by its backbone and can adopt a favorable conformation when binding to a surface. Similarly, architectures with fewer longer branches (SB1 and LC1) are qualitatively intermediate in performance when compared with architectures containing numerous shorter branches (SC1 and LC3). Finally, the star (S1) polymer with six short arms, emanating from a single branching point, would be expected to have the least freedom of movement and have the greatest difference when compared to the linear polymer for particle adsorption.

When compared to the DP_{30} series, the influence of architecture on the performance of the DP_{60} and DP_{120} materials was

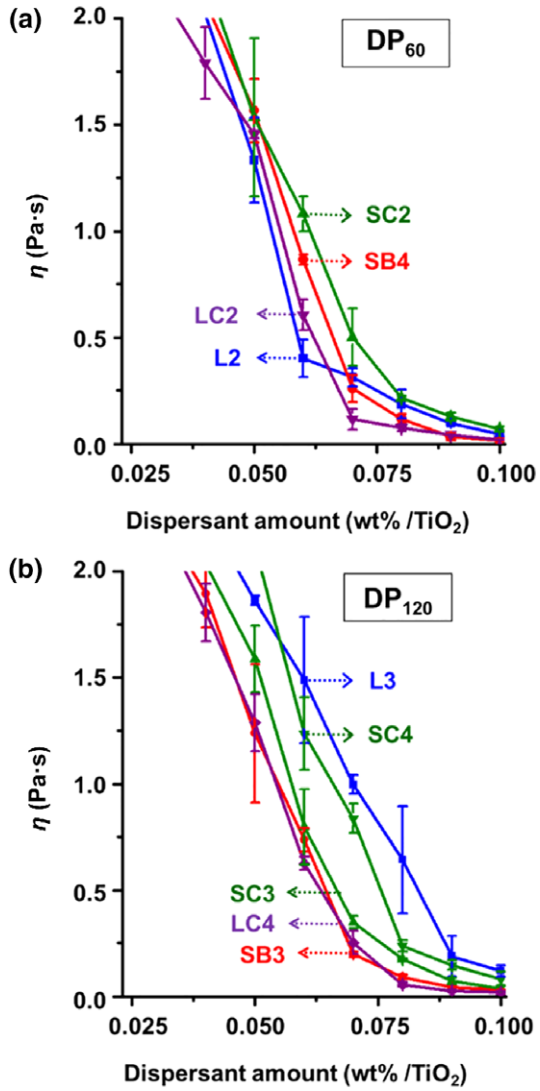

FIGURE 7 Dispersant demand plots of aqueous TiO_2 dispersions versus PAA dispersant amount. (a, b) Effect of architecture within the same DP_{60} and DP_{120} series, respectively. Viscosities were measured at a constant shear rate of 100 s^{-1}. [Color figure can be viewed at wileyonlinelibrary.com]

distinctly different (Fig. 7). In the case of the DP_{60} materials, the variation between the linear polymer (L2) and other architectures in reducing the viscosity of TiO_2 dispersion was less than for the DP_{30} series, potentially due to the longer branches interacting more efficiently with the TiO_2 particle surface. In direct contrast, for the DP_{120} materials, the branched architectures consistently performed better than the linear polymer (L3), highlighting the importance of branching, as opposed to the total molecular weight of the polymer at higher DP_n. This subtle interplay between branching and molecular weight is intriguing and suggests design principles governed by specific properties and performance requirements.

For industrial dispersant applications, the use of higher molecular weight dispersants is often desirable in commercial paint formulations as these are less readily displaced from the pigment surface by other additives. However, as previously discussed, high molecular weight linear dispersants will bridge particles, encouraging flocculation and increasing dispersion viscosity. In analyzing the structure–property relationships for the DP_{30}, DP_{60}, and DP_{120} series, the introduction of branches into a dispersant of comparable molecular weight reduces the resulting dispersant viscosity without compromising the number of possible surface binding sites. A rationale for the observed change in viscosity with branching at constant DP_n is that the introduction of branches reduces the maximum linear extension of the polymer, thereby preventing bridging between particles and encouraging primarily *intra*-particle adsorption. This concept introduces an additional parameter (architecture) for dispersant design, where the length of each branch can be tailored to fall within the range of the highest performing linear dispersants ($DP_1 < x < DP_{30}$, Figure 3). Lower molar mass branches would provide increased steric mobility and conformability to the TiO_2 particle surface with the added benefit of an overall higher molecular weight dispersant achieving an enhanced stability to additives. Accordingly, a subset of the branched DP_{120} architectures identified by this study (e.g., SB3, SC3, and LC4) show a significantly reduced pigment dispersion viscosity and improved performance when compared to L3 and other traditional linear PAA systems.

CONCLUSIONS

In summary, the synthesis of a library of well-defined PAA architectures based on the commercially important building block, acrylic acid, is reported. A statistical DoE model was used to identify target polymer architectures, with the aim of maximizing the structural space that could be experimentally investigated. Employing a combination of established strategies and new synthetic methodologies, linear, single branched, precision-branched comb, and star polymers were prepared. From these macromolecular isomers, the role of structure on dispersant performance was evaluated. Specifically, the PAA architectures were investigated as polymer additives for the dispersion for TiO_2 pigment particles. Using a combination of rheology and ITC measurements, important structural trends were identified leading to enhanced performance as TiO_2 dispersants. Significantly, we identified polymer architectures that show promise as next generation pigment dispersants and highlighted the role of polymer architecture in controlling properties. We anticipate that this work will guide the design of new, robust and industrially viable polymerization chemistries that improve material performance through architectural control.

ACKNOWLEDGMENTS

We thank the NSF Graduate Research Fellowship program and the Dow Chemical Company for financial support. A.A. (705041) and D.J.L. (657650) are grateful to the European Union's Horizon 2020 research and innovation programme for Marie Curie Global Fellowships. S.S. was supported by the National Research Foundation of Korea (NRF) grant funded by the Korea government (2017R1C1B5018327). A.A. acknowledges the California

NanoSystems Institute for an Elings Prize Fellowship. The research reported here made use of shared facilities of the UCSB MRSEC funded by the National Science Foundation (NSF DMR 1720256), a member of the Materials Research Facilities Network (www.mrfn.org). We also thank Dr. Rachel Behrens for assistance with polymer characterization.

REFERENCES AND NOTES

1 J. L. Freyer, S. D. Brucks, L. M. Campos, *J. Polym. Sci., Part A: Polym. Chem.* **2017**, *55*, 3167.

2 B. I. Voit, A. Lederer, *Chem. Rev.* **2009**, *109*, 5924.

3 G. Polymeropoulos, G. Zapsas, K. Ntetsikas, P. Bilalis, Y. Gnanou, N. Hadjichristidis, *Macromolecules* **2017**, *50*, 1253.

4 Y. Zeng, Q. Mahmood, T. Liang, W.-H. Sun, *J. Polym. Sci., Part A: Polym. Chem.* **2017**, *55*, 3214.

5 M. J. Maher, H. J. Schibur, F. S. Bates, *J. Polym. Sci., Part A: Polym. Chem.* **2017**, *55*, 3097.

6 Y. Ren, Z. Wei, X. Leng, T. Wu, Y. Bian, Y. Li, *J. Phys. Chem. B* **2016**, *120*, 4078.

7 R. D. McCullough, S. Tristram-Nagle, S. P. Williams, R. D. Lowe, M. Jayaraman, *J. Am. Chem. Soc.* **1993**, *115*, 4910.

8 T. Debuissy, E. Pollet, L. Avérous, *J. Polym. Sci., Part A: Polym. Chem.* **2017**, *55*, 2738.

9 R. Belibel, C. Barbaud, *J. Polym. Sci., Part A: Polym. Chem.* **2017**, *55*, 2408.

10 E. Girard, T. Tassaing, J.-D. Marty, M. Destarac, *Chem. Rev.* **2016**, *116*, 4125.

11 M. D. Malinsky, K. L. Kelly, G. C. Schatz, R. P. Van Duyne, *J. Am. Chem. Soc.* **2001**, *123*, 1471.

12 L. R. Middleton, E. B. Trigg, E. Schwartz, K. L. Opper, T. W. Baughman, K. B. Wagener, K. I. Winey, *Macromolecules* **2016**, *49*, 8209.

13 A. Gregory, M. H. Stenzel, *Prog. Polym. Sci.* **2012**, *37*, 38.

14 M. M. Obadia, S. Fagour, Y. S. Vygodskii, F. Vidal, A. Serghei, A. S. Shaplov, E. Drockenmuller, *J. Polym. Sci., Part A: Polym. Chem.* **2016**, *54*, 2191.

15 J. Lawrence, S.-H. Lee, A. Abdilla, M. D. Nothling, J. M. Ren, A. S. Knight, C. Fleischmann, Y. Li, A. S. Abrams, B. V. K. J. Schmidt, M. C. Hawker, L. A. Connal, A. J. McGrath, P. G. Clark, W. R. Gutekunst, C. J. Hawker, *J. Am. Chem. Soc.* **2016**, *138*, 6306.

16 J. Xu, C. Fu, S. Shanmugam, C. J. Hawker, G. Moad, C. Boyer, *Angew. Chem., Int. Ed.* **2017**, *129*, 8496.

17 S. Farrokhpay, *Adv. Colloid Interface Sci.* **2009**, *151*, 24.

18 L. T. Lee, P. Somasundaran, *Langmuir* **1989**, *5*, 854.

19 K. Esumi, H. Toyoda, T. Suhara, H. Fukui, *Colloids Surf., A* **1998**, *145*, 145.

20 S. Farrokhpay, G. E. Morris, D. Fornasiero, P. Self, *J. Colloid Interface Sci.* **2004**, *274*, 33.

21 J. Hwang, Y. Choe, J. Bang, A. Khan, *J. Polym. Sci., Part A: Polym. Chem.* **2017**, *55*, 3381.

22 J. L. Deiss, P. Anizan, S. El Hadigui, C. Wecker, *Colloids Surf. A* **1996**, *106*, 59.

23 S. Chibowski, M. Paszkiewicz, *Adsorpt. Sci. Technol.* **2001**, *19*, 397.

24 F. Nsib, N. Ayed, Y. Chevalier, *Prog. Org. Coat.* **2007**, *60*, 267.

25 S. Farrokhpay, G. E. Morris, D. Fornasiero, P. Self, *Colloids Surf. A* **2005**, *253*, 183.

26 A. Hirao, K. Murano, T. Oie, M. Uematsu, R. Goseki, Y. Matsuo, *Polym. Chem.* **2011**, *2*, 1219.

27 C. J. Hawker, A. W. Bosman, E. Harth, *Chem. Rev.* **2001**, *101*, 3661.

28 J. Chiefari, Y. K. Chong, F. Ercole, J. Krstina, J. Jeffery, T. P. T. Le, R. T. A. Mayadunne, G. F. Meijs, C. L. Moad, G. Moad, E. Rizzardo, S. H. Thang, *Macromolecules* **1998**, *31*, 5559.

29 J.-S. Wang, K. Matyjaszewski, *J. Am. Chem. Soc.* **1995**, *117*, 5614.

30 M. Kato, M. Kamigaito, M. Sawamoto, T. Higashimura, *Macromolecules* **1995**, *28*, 1721.

31 B. Wenn, A. C. Martens, Y.-M. Chuang, J. Gruber, T. Junkers, *Polym. Chem.* **2016**, *7*, 2720.

32 A. Muehlebach, F. Rime, *J. Polym. Sci., Part A: Polym. Chem.* **2003**, *41*, 3425.

33 J. M. Ren, J. T. Wiltshire, A. Blencowe, G. G. Qiao, *Macromolecules* **2011**, *44*, 3189.

34 C. J. Duxbury, D. Cummins, A. Heise, *J. Polym. Sci., Part A: Polym. Chem.* **2009**, *47*, 3795.

35 Z. A. Page, R. Bou Zerdan, W. R. Gutekunst, A. Anastasaki, S. Seo, A. J. McGrath, D. J. Lunn, P. G. Clark, C. J. Hawker, *J. Polym. Sci., Part A: Polym. Chem.* **2017**, *55*, 801.

36 J. R. Finnegan, D. J. Lunn, O. E. C. Gould, Z. M. Hudson, G. R. Whittell, M. A. Winnik, I. Manners, *J. Am. Chem. Soc.* **2014**, *136*, 13835.

37 P. J. M. Stals, Y. Li, J. Burdyńska, R. Nicolaÿ, A. Nese, A. R. A. Palmans, E. W. Meijer, K. Matyjaszewski, S. S. Sheiko, *J. Am. Chem. Soc.* **2013**, *135*, 11421.

38 J. T. Trotta, M. Jin, K. J. Stawiasz, Q. Michaudel, W. L. Chen, B. P. Fors, *J. Polym. Sci., Part A: Polym. Chem.* **2017**, *55*, 2730.

39 J. M. Ren, T. G. McKenzie, Q. Fu, E. H. H. Wong, J. Xu, Z. An, S. Shanmugam, T. P. Davis, C. Boyer, G. G. Qiao, *Chem. Rev.* **2016**, *116*, 6743.

40 W. R. Gutekunst, A. Anastasaki, D. J. Lunn, N. P. Truong, R. Whitfield, G. R. Jones, N. J. Treat, A. Abdilla, B. E. Barton, P. G. Clark, D. M. Haddleton, T. P. Davis, C. J. Hawker, *Macromol. Chem. Phys.* **2017**, *218*, 1700107.

41 S. Liufu, H. Xiao, Y. Li, *J. Colloid Interface Sci.* **2005**, *281*, 155.

42 J. Loiseau, N. Doërr, J. M. Suau, J. B. Egraz, M. F. Llauro, C. Ladavière, J. Claverie, *Macromolecules* **2003**, *36*, 3066.

43 J. Chen, T. He, W. Wu, D. Cao, J. Yun, C. K. Tan, *Colloids Surf. A* **2004**, *232*, 163.

44 C. R. Kothapalli, M. Wei, M. T. Shaw, *Soft Matter* **2008**, *4*, 600.

45 Y. Shi, Y. Wu, J. Li, G. Li, *J. Dispers. Sci. Technol.* **2003**, *24*, 739.

46 S. G. J. Heijman, H. N. Stein, *Langmuir* **1995**, *11*, 422.

47 Q. Ran, S. Wu, J. Shen, *Polym. Plast. Technol. Eng.* **2007**, *46*, 1117.

48 J. Blaakmeer, M. R. Bohmer, M. A. C. Stuart, G. J. Fleer, *Macromolecules* **1990**, *23*, 2301.

49 J. Cesarano, I. A. Aksay, *J. Am. Ceram. Soc.* **1988**, *71*, 1062.

50 A. Pettersson, G. Marino, A. Pursiheimo, J. B. Rosenholm, *J. Colloid Interface Sci.* **2000**, *228*, 73.

51 L. Wu, Y. Huang, Z. Wang, L. Liu, *J. Eur. Ceram. Soc.* **2010**, *30*, 1327.

52 Y. K. Leong, P. J. Scales, T. W. Healy, D. V. Boger, *Colloids Surf. A* **1995**, *95*, 43.

53 F. Karakaş, M. S. Çelik, *Colloids Surf. A* **2013**, *434*, 185.

54 J.-P. Boisvert, J. Persello, A. Foissy, J.-C. Castaing, B. Cabane, *Colloids Surf. A* **2000**, *168*, 287.

55 B. C. Ong, Y. K. Leong, S. B. Chen, *Powder Technol.* **2008**, *186*, 176.

56 J.-P. Boisvert, J. Persello, J.-C. Castaing, B. Cabane, *Colloids Surf. A* **2001**, *178*, 187.

57 P. L. Golas, S. Louie, G. V. Lowry, K. Matyjaszewski, R. D. Tilton, *Langmuir* **2010**, *26*, 16890.

58 J. J. Florio, D. J. Miller, *Handbook of Coating Additives*, 2nd ed.; CRC Press, New York, NY, **2004**.

59 C. Geffroy, J. Persello, A. Foissy, P. Lixon, F. Tournilhac, B. Cabane, *Colloids Surf. A* **2000**, *162*, 107.

60 F. Loosli, L. Vitorazi, J.-F. Berret, S. Stoll, *Environ. Sci.: Nano* **2015**, *2*, 541.

61 F. Loosli, L. Vitorazi, J.-F. Berret, S. Stoll, *Water Res.* **2015**, *80*, 139.

62 K. Chiad, S. H. Stelzig, R. Gropeanu, T. Weil, M. Klapper, K. Müllen, *Macromolecules* **2009**, *42*, 7545.